PNAS
www.pnas.org

Supplementary Information for

RIG-I regulates myeloid differentiation by promotingTRIM25-mediated ISGylation

Song-Fang Wu[a,b,1], Li Xia [a,1], Xiao-Dong Shi[a], Yu-Jun Dai[a], Wei-Na Zhang[a], Jun-Mei Zhao[a], Wu Zhang[a], Xiang-Qin Weng[a], Jing Lu[a], Huang-Ying Le[b], Sheng-ce Tao[b], Jiang Zhu[a], Zhu Chen[a,b,2], Yue-Ying Wang[a,2], and Saijuan Chen[a,b,2]

[a]State Key Laboratory of Medical Genomics, Shanghai Institute of Hematology, National Research Center for Translational Medicine at Shanghai, Rui Jin Hospital affiliated to Shanghai Jiao Tong University School of Medicine, Shanghai 200025, China; and [b]Key Laboratory of Systems Biomedicine (Ministry of Education), Shanghai Center for Systems Biomedicine, Shanghai Jiao Tong University, 800 Dongchuan Road, Shanghai 200240, China

[1] S.-F.W. and L.X. contributed equally to this work.

[2] To whom correspondence may be addressed. Email: zchen@stn.sh.cn, yywang@shsmu.edu.cn, or sjchen@stn.sh.cn.

This PDF file includes:

Other supplementary materials for this manuscript include the following:

www.pnas.org/cgi/doi/10.1073/pnas.1918596117

Supplementary text

Supplementary Materials and Methods

RIP-seq and Data Analysis

RNA-binding protein immunoprecipitation (RIP) was performed with an EZ-Magna RIP Kit. First, NB4 cells were induced to differentiation with RIG-I upregulation by 3 d treatment with 1 μM ATRA. Next, 3×10^7 cells were lysed by RIP lysis buffer and frozen overnight at -80 ℃. Then, immunoprecipitation (IP) was performed using anti-RIG-I N-terminus antibodies or immunoglobulin G as negative control, and the antibody-enriched RNAs were extracted and purified after digestion of DNA and proteins. These enriched and purified RNAs and input RNA were subject to analysis by high-throughput sequencing (KangChen Bio-tech Inc). Human genome was used for calculating the RNA expression level and annotating RNAs. RNA expression level (FPKM value) was calculated using Cufflink2 software (version 2.1.1). RIG-I binding RNAs were defined only if they met three conditions: IP / IgG > 2, Input > 0, and IP / Input > 1. A total of 1,765 transcripts were identified, among which 1,540 were protein-coding genes.

We used STRING (version 11.0) (1) for functional enrichment analysis and screening of the RIG-I binding gene as shown by the workflow in Figure S1. First, 1,540 protein-coding genes were inputted to STRING to carry on gene ontology enrichment analysis. Second, to explore the most relevant pathways and genes associated with RIG-I, we analyzed the protein-protein association network between RIG-I and the 149 genes enriched in the immune-related pathway with the lowest *P* value (GO: 0002252, immune effector process) using confidence model of network edges. The network was clustered using k-means clustering algorithm, which identified a relatively independent gene cluster composed of 16 genes associated with RIG-I. The protein-protein interaction analysis was then performed using molecular action of network edges to zoom in the cluster and to find the most relevant genes.

RNA Pull-down Assay

RNA pull-down assays were performed with a Pierce Magnetic RNA-Protein Pull-Down Kit (2). In brief, the fragments of *TRIM25* RNA were transcribed and labeled with biotin. To produce 5′ m^7G analog capped RNA, we added the m^7G analog (Promega) in the transcriptional system (3). The uncapped RNAs were successively digested by 5′ polyphosphatase and terminator 5′-phosphate-dependent exonuclease. Then, 1×10^7 NB4 cells were collected and lysed by IP lysis

buffer, and a pull-down assay was performed with 50 pmol biotin-labeled RNA or poly(A) as negative control. Immunoblotting was used to detect the interaction between the RIG-I and *TRIM25* RNA.

Kinetic Binding Experiments

The affinity constants for the interaction between the domains of RIG-I and the *TRIM25* RNA fragments were measured with Octet Red 96 (Pall ForteBio) (4). Using a protein purification system, the GST fusion proteins were purified from *Escherichia coli* BL21 (DE3), transformed by plasmids carrying the various domains of RIG-I, and induced by 0.5 mM IPTG at 16 ℃ overnight. The RNAs were transcribed and labeled with biotin at the 3′ end as described above. We captured the biotin-RNA with a streptavidin biosensor and measured the association and dissociation curves in real time for the RNA with various concentrations of protein in phosphate-buffered saline/Tween (pH 8.0, 0.02% Tween-20) with Octet Red 96 (4). Octet System Data Analysis 7.1 was used to fit the affinity constants for the interactions (K_{on}, K_{off}, and K_D) using a 1:1 model.

Transfection and Lentiviral Infection

Lentiviral particles for luciferase assay were packaged in HEK 293T cells by cotransfection of pLVX-Metluc carrying the DNA fragments near the transcription initiation site of *TRIM25* gene and packaging plasmids psPAX2 and pMD2.G as previously described (5). Virus in supernatant was collected 48–72 hours after transfection. NB4 and U937-RIG-I cells were infected by incubating with the lentivirus and polybrene for 24 hours at 37 ℃ and selected by puromysin. For knockdown of TRIM25 and ISG15, lentiviral particles were packaged in HEK 293T cells by cotransfecting pLVX-shRNA2, psPAX2 and pMD2.G, and the positive cells were sorted by flow cytometry.

Luciferase Assay

NB4 and U937-RIG-I cells stably expressing *Metridia* luciferase were induced by ATRA for 3 d and doxycycline depletion for 5 d, respectively. And then, the control and induced cells collected and lysised by passive lysis buffer. *Metridia* luciferase activity of the lysate was detected using coelenterazine in Dual-Luciferase Reporter Assay System. Protein quantity of lysate was measured by Pierce BCA Protein Assay Kit. The *Metridia* luciferase activity of the induced cells was standardized by protein concentration and normalized by the activity of control cells. The relative luciferase activity of each group compared with vector was shown.

To explore the domains of RIG-I regulating the transcriptional activity of *TRIM25*, the plasmids pRL-SV40, pflag-CMV4-RIG-I domains, and the pGL4·15 plasmid containing the promoter DNA fragment of *TRIM25* were co-transfected into HEK 293T cells using polyethylenimine. After 24-hour transfection, the cells were collected, and the *Firefly* luciferase and *Renilla* luciferase activities of each group were measured. After normalization according to the *Renilla* luciferase activity, the relative luciferase activity of each group was calculated.

RNA Stability Assay

NB4 cells were treated with 5 μg/mL ActD before and after the 3 d treatment with 1 μM ATRA. Cells were collected at different time points upon ActD treatment. Quantitative RT-qPCR was used to detect the relative expression level of *TRIM25* mRNA at various time points. The mRNA expression levels of TRIM25 were also assayed in U937-RIG-I cells before and after the 5 d induction of RIG-I followed by the treatment of 5 μg/mL ActD. The HEK 293T cells were transfected with pflag-CMV4 plasmid constructed with the full length or domains of RIG-I. After 24-hour transfection, cells were treated with 5 μg/mL ActD and collected at different time points upon ActD treatment. *P*-values were calculated by performing paired t-tests.

Flow Cytometry Analysis

The NB4 cells with TRIM25 or ISG15 knockdown were treated with 1 μM ATRA for 3 d. To induce the expression of RIG-I, doxycycline was removed from the medium of U937-RIG-I cells with TRIM25 or ISG15 knockdown for 5 d. Then, 1×10^5 cells were collected and incubated with fluorescein isothiocyanate-labeled anti-CD11b antibodies and analyzed by a BD FACS Calibur analyzer. Phagocytosis assay was performed as previously reported (5). Briefly, NB4 cells were collected and incubated with serum-opsonized fluorescent microspheres for 2 hours at 37 ℃. The percentage of fluorescent cells was assayed by flow cytometry.

Cell Culture and Staining

RIG-I inducible cell line U937-RIG-I was produced as described in our previous work (6). U937-RIG-I cells were cultured in RPMI-1640 supplemented with 10% (vol/vol) fetal bovine serum (FBS) and incubated in 5% CO_2 at 37 ℃. Usually, 2 μg/mL of doxycycline was added to the medium to inhibit RIG-I expression. Depletion of doxycycline can induce RIG-I expression. NB4 cells were cultured in RPMI-1640 supplemented with 10% FBS and incubated in 5% CO_2 at 37 ℃. 1 μM ATRA was added into medium of NB4 cells for inducing differentiation. HEK 293T cells

were cultured in DMEM supplemented with 10% FBS and incubated in 5% CO_2 at 37 ℃. Wright-Giemsa staining was performed to observe the morphological changes.

Plasmids Construction

Plasmids used in transcription for TRIM25, recombinant expression for RIG-I domains, flag-tagged RIG-I domains, luciferase for TRIM25 promoter, and shRNA for RIG-I, TRIM25, ISG15 and STAT1 were constructed by standard molecular biology technique. The sequences targeted for shRNA were listed in *SI Appendix*, Table S2.

RNA Isolation, Reverse Transcription, and RT-qPCR

Cellular total RNAs were extracted from the cells with TRIzol, and the antibody-enriched RNAs in the RIP experiments were extracted with phenol: chloroform: isoamyl alcohol (25:24:1, v/v). The purified RNAs were reversely transcribed into cDNA using a reverse transcription kit (Invitrogen). RT-qPCR was performed using 7500 Real-Time PCR System, and the data from biological replicates were plotted as mean ± SEM. The gene-specific primers were listed in *SI Appendix*, Table S3.

Immunoblot Analysis

Cells were lysed by SDS lysis buffer (Beyotime) and boiled for 10 minutes. Whole-cell lysates were quantified and separated by sodium dodecyl sulfate–polyacrylamide gel electrophoresis and transferred to 0.45 μm PVDF membranes (Amersham Hybond). The membranes were locked in 5% skimmed milk powder, and then incubated with primary antibodies overnight at 4 ℃. Immunodetection was performed using chemiluminescence western blotting substrate.

Supplementary Figures and Legends

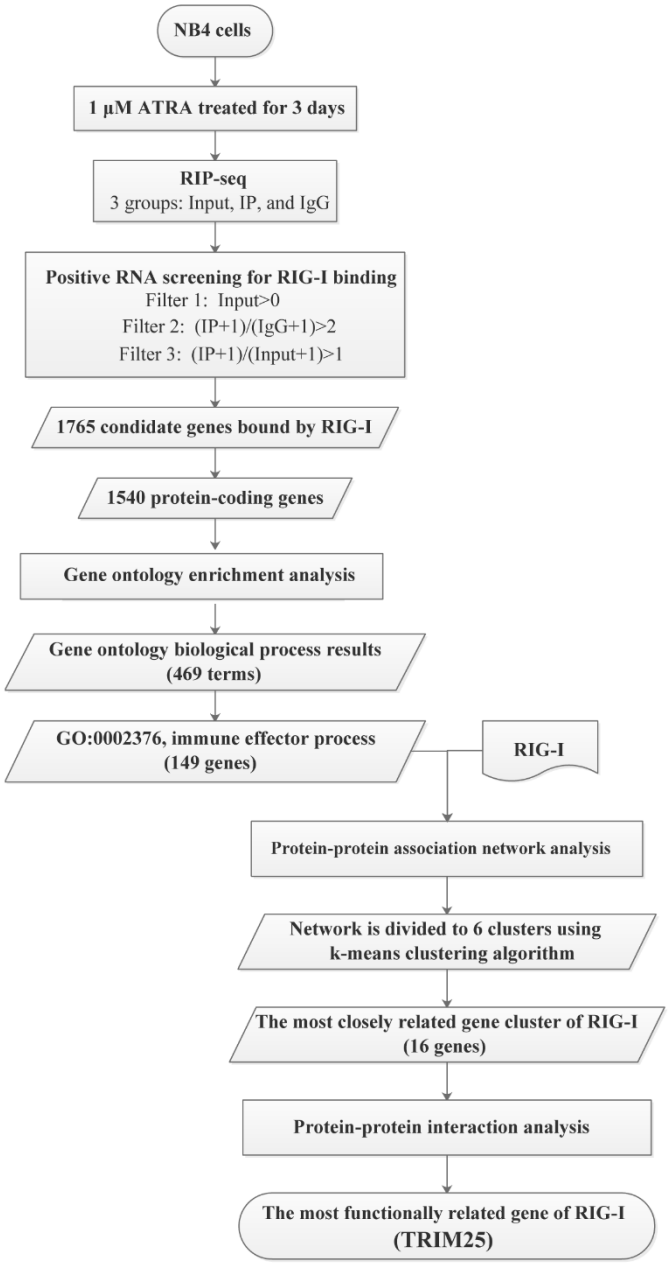

Fig. S1 The workflow of RIP-seq data analysis.

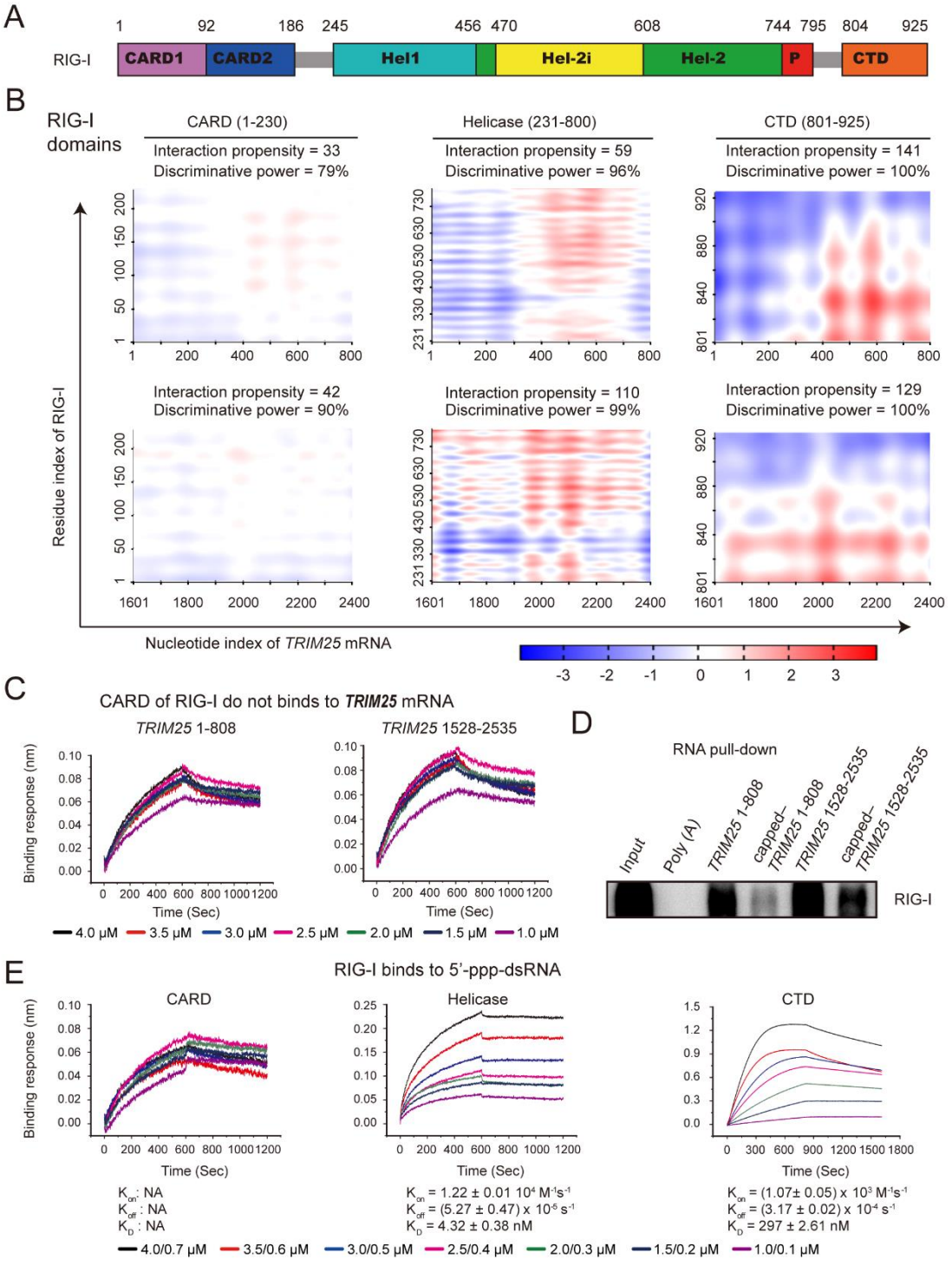

Fig. S2 RIG-I binds RNA of TRIM25 gene cluster.

(*A*) Schematic diagram of RIG-I protein.

(*B*) Matrix map of the interaction between the residues of RIG-I and nucleotides of *TRIM25* mRNA predicted by *cat*RAPID strength analysis. Interaction propensity indicates the propensity of

proteins to interact with RNA. Discriminative power is a value to evaluate the ability of *cat*RAPID to distinguish between interacting and non-interacting RNA-protein associations.

(*C*) Binding kinetic assay showed the CARD of RIG-I could not bind *TRIM25* mRNA by using Bio-layer interferometry (BLI) technique.

(*D*) RNA pulldown showed the interaction between RIG-I and *TRIM25* mRNA was not dependent on 5' triphosphate.

(*E*) The interaction between RIG-I and 5'ppp-dsRNA. BLI technique was used to measure the kinetic constants of the interaction between 5'ppp-dsRNA and different domains of RIG-I.

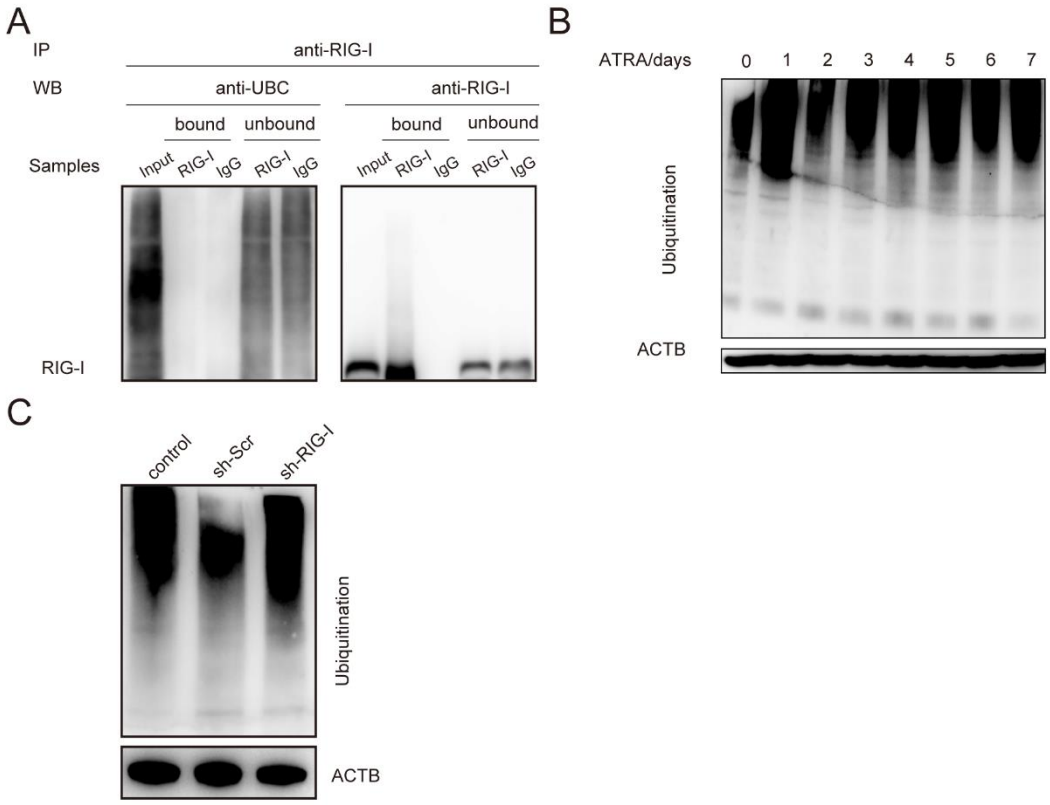

Fig. S3 The ubiquitination of RIG-I and overall ubiquitination have no obvious change during ATRA induced differentiation.

(*A*) Immunoprecipitation and immunoblotting were performed to test the ubiquitination of RIG-I in NB4 cells with ATRA induction. (Bound: beads-enriched sample; unbound: supernatant sample.)

(*B*) ATRA induction had no effect on the total ubiquitination in NB4 cells.

(*C*) RIG-I knockdown by shRNA did not affect the total ubiquitination of in NB4 cells after treatment with 1 μM ATRA for 3 d.

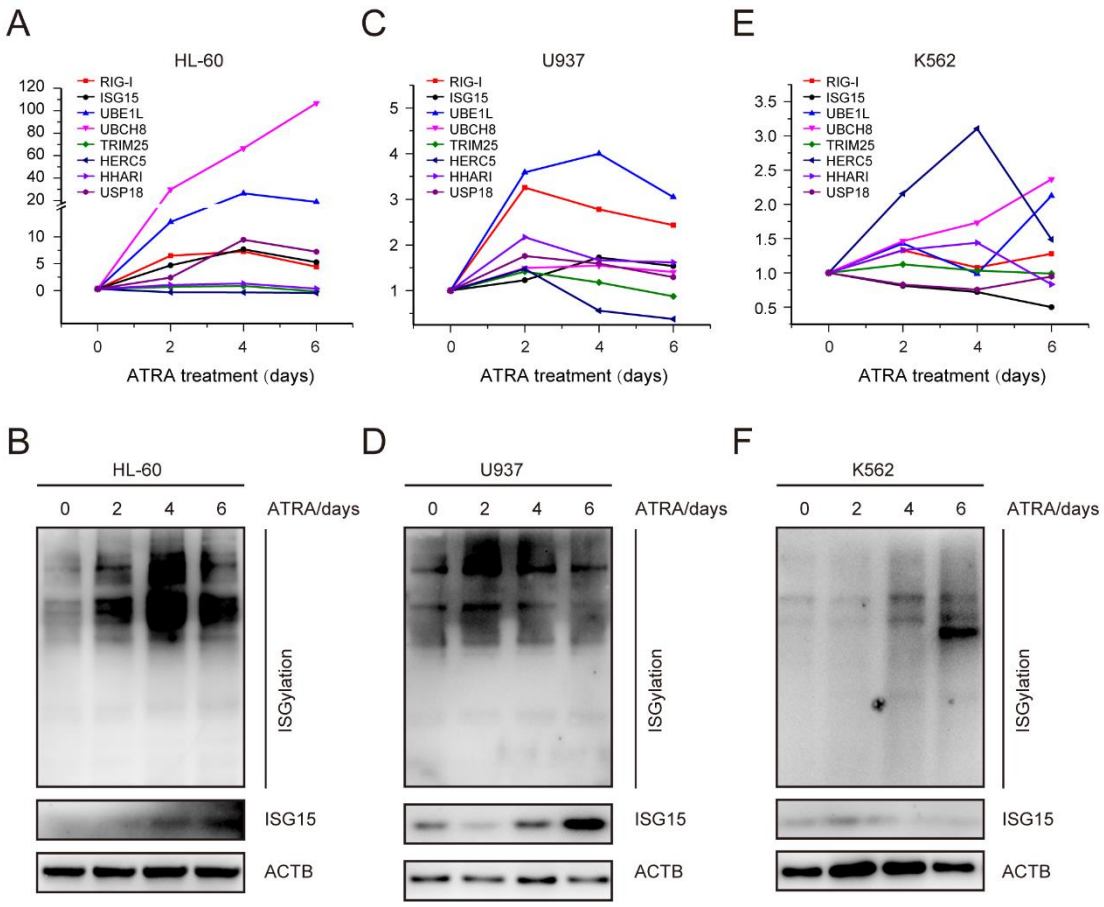

Fig. S4 Upregulation of ISGylation by ATRA treatment in myeloid leukemia cells.

(*A*-*B*) ATRA induced the expression of ISGylation pathway genes and the overall ISGylation modification level in HL-60 cells. HL-60 cells were collected at various time points after the treatment with 2 μM ATRA. The expression levels of the mRNAs of ISGylation genes (A) and the ISGylation modification (B) were evaluated respectively.

(*C*-*F*) ATRA induced the expression of ISGylation pathway genes and the overall ISGylation modification level in U937 (C and D) and K562 (E and F) cells. The concentration of ATRA and cell collection time points were the same as those in HL-60 cells.

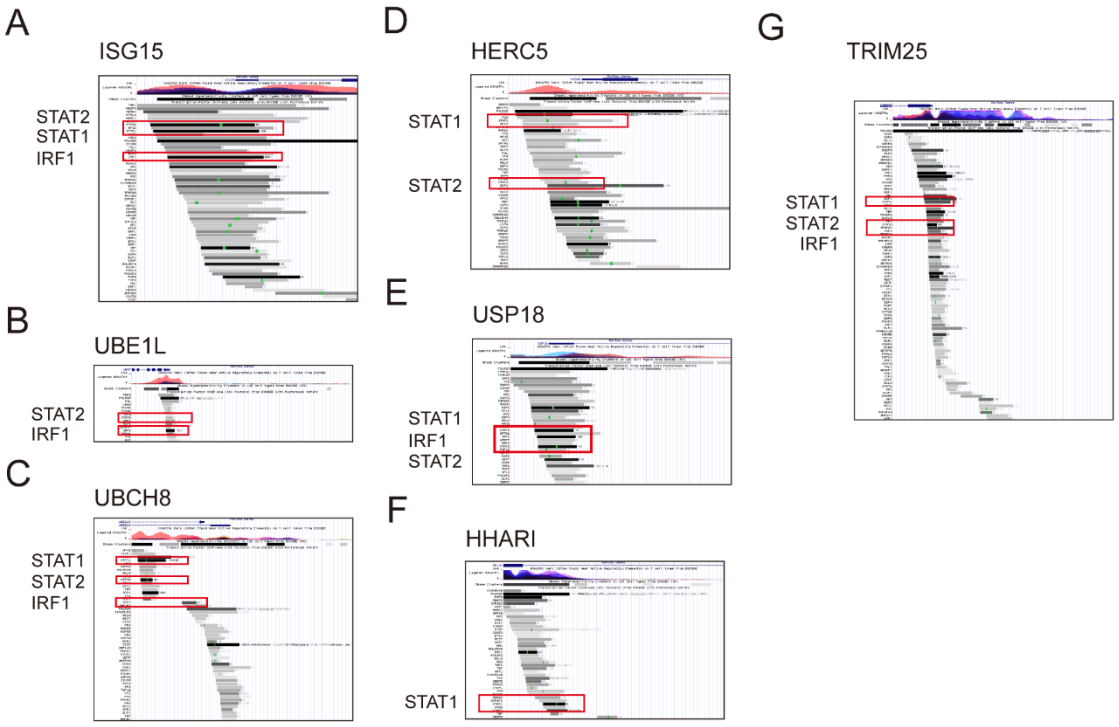

Fig. S5 The binding motifs of STAT1, STAT2, and IRF1 located in the promoter of ISGylation pathway genes.

(*A*-*G*) Screenshots show the binding motifs of STAT1, STAT2, and IRF1 located in the promoter of ISGylation pathway genes according to the ENCODE database.

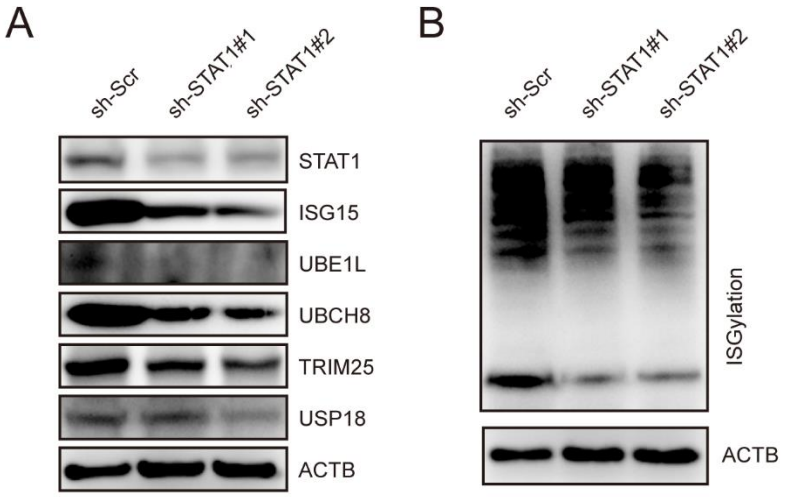

Fig. S6 Knockdown of STAT1 downregulated the ISGylation pathway genes and reduced total ISGylation.

(*A*-*B*) Knockdown of STAT1 downregulated the ISGylation pathway genes (A) and the overall ISGylation modification level (B) in NB4 cells after treatment with ATRA at 1 μM for 3 d.

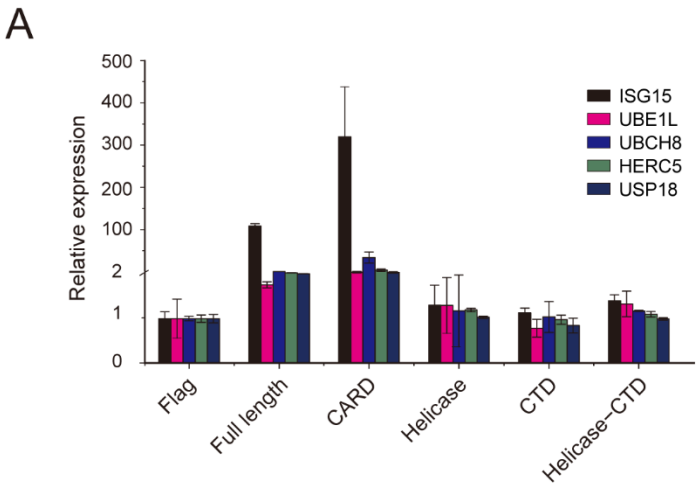

Fig. S7 RIG-I promoted the expression of the ISGylation pathway genes via the CARD domain in HEK 293T cells.

(*A*) HEK 39T cells transfected with pflag-CMV4 plasmids constructed with the full length or different domains of RIG-I. After 24-hour transfection, cells were collected for RNA extraction and quantitative RT-qPCR of ISGylation pathway genes.

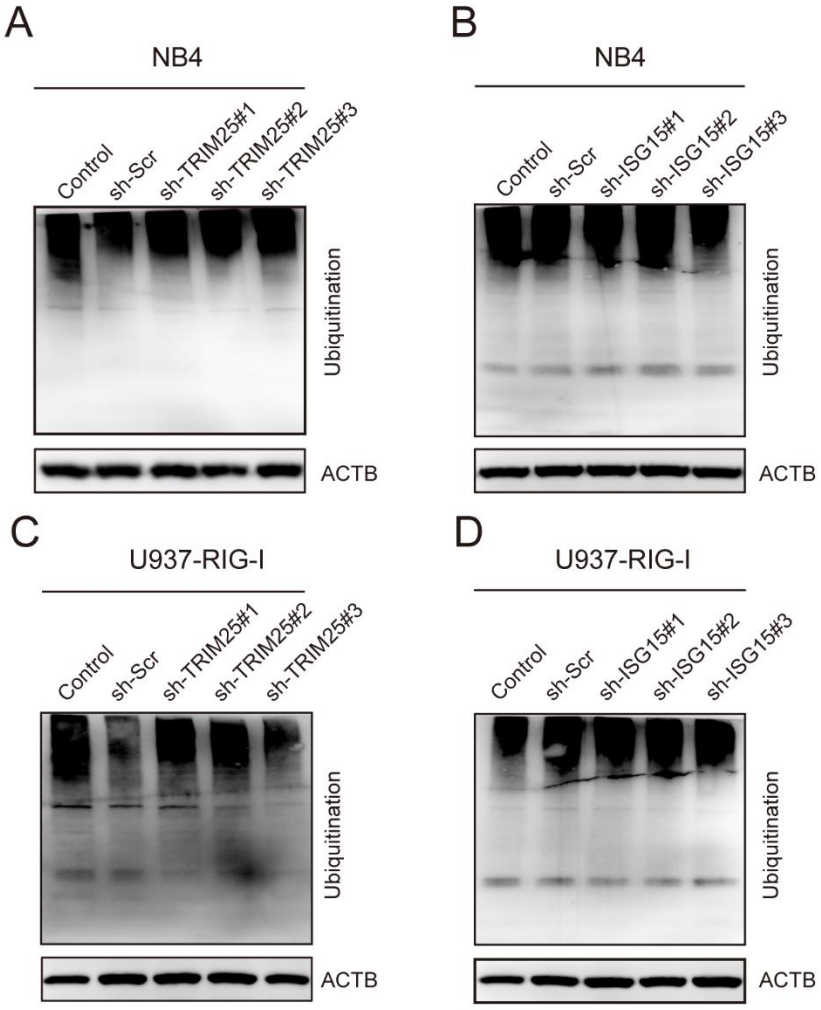

Fig. S8 Knockdown of TRIM25 or ISG15 has no effect on the total ubiquitination in NB4 and U937-RIG-I cells.

(*A-B*) The knockdown of TRIM25 or ISG15 in NB4 cells did not affect the total ubiquitination. Immunoblotting was used to detect ubiquitination status in NB4 cells with TRIM25 (A) or ISG15 (B) knockdown after 3 d of treatment with 1 μM ATRA.

(*C-D*) TRIM25 or ISG15 knockdown in U937-RIG-I cells did not affect the total ubiquitination. Immunoblotting was used to detect ubiquitination levels in U937-RIG-I cells with TRIM25 (C) or ISG15 (D) knockdown after 5 d of culture with depletion of doxycycline.

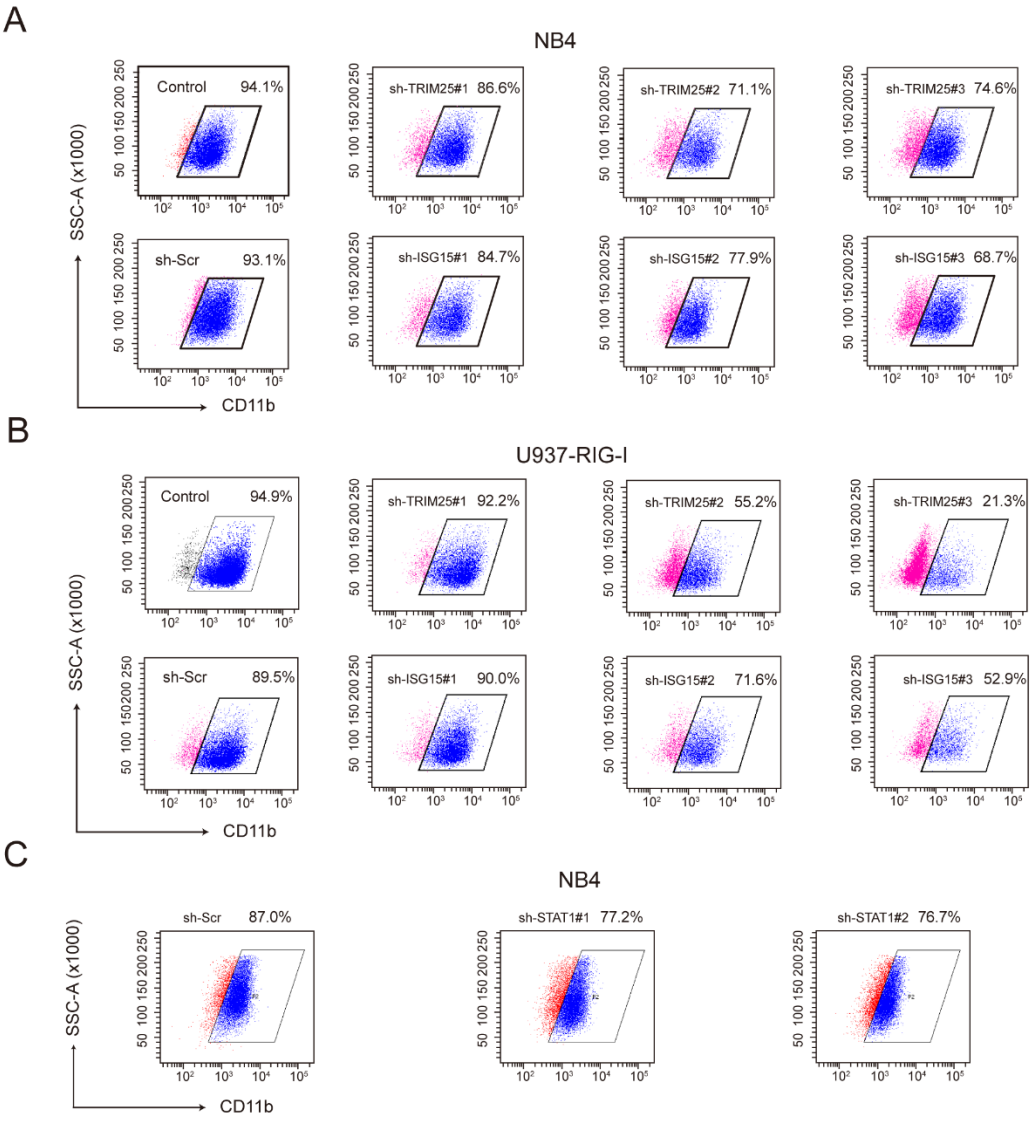

Fig. S9 Knockdown of TRIM25, ISG15 or STAT1 inhibits myeloid differentiation.

(*A*) Knockdown of TRIM25 or ISG15 in NB4 cells inhibited CD11b expression. Flow cytometry analysis was used to detect CD11b expression in NB4 cells with TRIM25 or ISG15 knockdown after the 3 d of treatment with 1 μM ATRA.

(*B*) Knockdown of TRIM25 or ISG15 in U937-RIG-I cells inhibited CD11b expression. Flow cytometry analysis was used to detect CD11b expression in U937-RIG-I cells with TRIM25 or ISG15 knockdown after doxycycline depletion for 5 d.

(*C*) Knockdown of STAT1 in NB4 cells inhibited CD11b expression. Flow cytometry analysis was used to detect CD11b expression in NB4 cells with STAT1 knockdown after the 3 d of treatment with 1 μM ATRA.

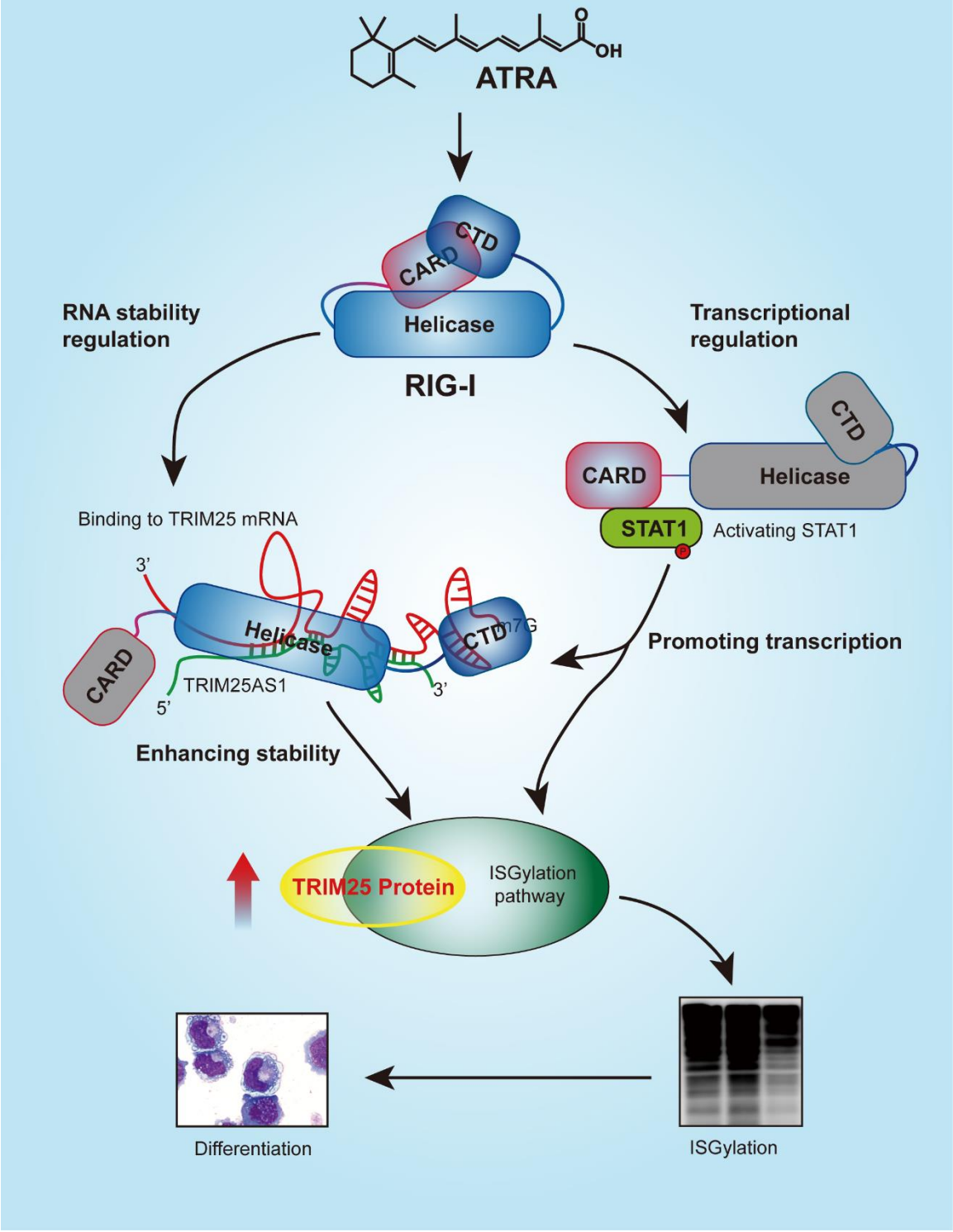

Fig. S10 Schematic diagram of RIG-I modulating myeloid differentiation through TRIM25 mediated ISGylation.

Supplementary Tables

Table S1. Key Resource Table.

REAGENT or RESOURCE	SOURCE	IDENTIFIER	Application
Antibodies			
Anti-RIG-I	Merck Millipore	06-1040	RIP, IP
Anti-RIG-I	Adipogen	AG-20B-0009-C100	WB, IP
Anti-TRIM25	BD	610570	WB
Anti-ISG15	Abclonal	A0154	WB
Anti-UBE1L	Proteintech	15818-1-AP	WB
Anti-UBCH8	Abclonal	A4282	WB
Anti-HERC5	Proteintech	22692-1-AP	WB
Anti-HHARI	Proteintech	14949-1-AP	WB
Anti-USP18	Proteintech	12153-1-AP	WB
Anti-STAT1	Proteintech	10144-2-AP	WB
Anti-STAT1-p701	Abclonal	AP0135	WB
Anti-STAT2	Proteintech	16674-1-AP	WB
Anti-STAT2-p690	Abclonal	AP0284	WB
Anti-IRF1	Proteintech	11335-1-AP	WB
Anti-Ubiquitin B	Proteintech	10201-2-AP	WB
Anti-ACTB	Proteintech	HRP-60008	WB
FITC Mouse anti-Human CD11b	BD	562793	Flow cytometry
PE Mouse Anti-Human CD11b	BD	561001	Flow cytometry
Chemicals			
Actinomycin D	Meilunbio	MB2221	RNA Stability
Ribo m7G Cap Analog	Promega	P1711	RNA capping
PureProteome™ Protein A/G Mix Magnetic Beads	Merck Millipore	LSKMAGAG02	RNA transcription
RNA 5 ´Polyphosphatase	Epicentre	RP8092H	RNA capping
Terminator™ 5´-Phosphate-Dependent Exonuclease	Epicentre	TER51020	RNA capping
IP lysis buffer	Thermo Fisher Scientific	87788	RNA pulldown; IP
Doxycycline	LabLife	631311	RIG-I induction
Effectene Transfection Reagent	Qiagen	301425	Transfection
Polyethylenimine	Sigma-Aldrich	408727-100ML	Transfection
Wright-Giemsa Dye Kit	BASO	BA4017	Wright-Giemsa staining
RNase Inhibitor	Ambion	AM2696	RNAse inhibitor
Protease Inhibitor Cocktail	Sigma-Aldrich	P8340-1ML	Protease Inhibitor

REAGENT or RESOURCE	SOURCE	IDENTIFIER	Application
Retinoic acid	Sigma-Aldrich	R2625	Differentiation induction
Latex beads, amine-modified polystyrene, fluorescent blue	Sigma-Aldrich	L0280	Phagocytosis assay
5'ppp-dsRNA	InvivoGen	tlrl-3prnalv-100	Kinetic assay
Critical Commercial Assay kits			
Magna RIP RNA-Binding Protein Immunoprecipitation Kit	Merck Millipore	17-701	RIP
Pierce Magnetic RNA-Protein Pull-Down Kit	Thermo Fisher Scientific	20164	RNA pulldown
Pierce™ RNA 3' End Desthiobiotinylation Kit	Thermo Fisher Scientific	20163	RNA labeling
RiboMAX™ Large Scale RNA Production Systems-T7	Promega	P1280	RNA transcription
Streptavidin Biosensors	Pall ForteBio	18-5019	Kinetic assay
Dual-luciferase Reporter Assay System	Promega	TM040	Transcriptional activities assay
Experimental models			
U937-RIG-I cell line	Our group (6)		Cell model
Softwares			
catRAPID	Gian Gaetano Tartaglia' lab	http://s.tartaglialab.com/page/catrapid_group	Prediction for RNA-protein interaction
ENCODE	ENCODE	http://genome.ucsc.edu/	Promoter assay
Data analysi 7.1	Pall ForteBio	https://www.fortebio.com/software-updates.html	Kinetic assay
Plasmids			
pGEX-4T-2			Fusion protein expression for RIG-I
pcDNA3.1			RNA transcription
pLVX-shRNA2			Knockdown
psPAX2			Lentiviral packaging
pMD2.G			Lentiviral packaging
pLVX-Metluc			Transcriptional activities assay
pGL4.15			Transcriptional activities assay
pRL-SV40			Transcriptional activities assay
pflag-CMV4			Overexpression

Table S2. Target Sequences for designing short hairpin RNA.

Name	Target sequence (cDNA, 5’ to 3’)
sh-TRIM25#1	GAGTGAGATCCAGACCTTGA
sh-TRIM25#2	GAACTGAACCACAAGCTGAT
sh-TRIM25#3	GTGCCCGATTCCTCTTAGAG
sh-ISG15#1	CATGTCGGTGTCAGAGCTGAA
sh-ISG15#2	AGCAGCGTCTGGCTGTCCA
sh-ISG15#3	GACCTGTTCTGGCTGACCTTC
sh-STAT1#1	CCCTGAAGTATCTGTATCCAA
sh-STAT1#2	CGACAGTATGATGAACACAGT
sh-RIG-I	CCACTTAAACCCAGAGACAAT

Table S3. Primers used for RT-qPCR analysis.

Gene Name	Forward sequence (5' to 3')	Reverse sequence (5' to 3')
NFKB1	AACTTGGCTTCCTTTCTTGGT	TAGTAAGCAACCTCATCCCCA
RIG-I	GGACGTGGCAAAACAAATCAG	GCAATGTCAATGCCTTCATCA
TRIM25	AAGTCATGAGTGCCCGATTCC	GCCCAAGACAGAACCTACAGT
ISG15	GCAGCGAACTCATCTTTGCCAGTA	AGGGACACCTGGAATTCGTTGC
UBE1L	ATCACTGAGGACCTGCTGTTGGACT	TCAGCCGCCAGAAAGCAAACT
UBCH8	TGTCCAGCGATGATGCCAATG	GGAAGCTGATGCGCAGGTTGA
HERC5	ATGGGCTGCTGTTTACTTTCG	GTCACTCTATACCCAACAAGCTCAG
HHARI	CACTTATGTCTTCGCTTTCTACCTC	GGGAAATATCTCGTTCAAGGTAGC
USP18	CCTAACTACCACTGGCAGGAAACTG	CCTAACTACCACTGGCAGGAAACTG
18sRNA	CGGCGACGACCCATTCGAAC	GAATCGAACCCTGATTCCCCGTC

Dataset S1. Lists of RIG-I binding RNAs.

Column A: GeneName, Name of the gene.

Column B: IP/IgG, The Fold Change of IP vs IgG. To avoid zero division, 1.0 was added. *i.e.* (IP+1)/(IgG+1).

Column C: IP/Input, The Fold Change of IP vs IgG. To avoid zero division, 1.0 was added. *i.e.* (IP+1)/(Input+1).

Column D-F: FPKM Value, FPKM of the RNA in all samples.

Column G: Biotype, gene was classificated as mRNA, miRNA, antisense, lincRNA, lncRNA (Array Star), snoRNA, snRNA, and others.

Column H: Gene_Description, description of the gene.

Column I: Locus, Genomic coordinates of the gene.

Column J: Strand, Strand of the gene.

Column K: Transcript_Length, length of the transcript.

Column L: ENSEMBL_Gene ID, ENSEMBL gene id of each gene.

Dataset S2. Lists of GO biological process enrichment for RIG-I binding protein-coding genes.

Dataset S3. STRING k-means clusters of RIG-I binding protein-coding genes in immune effector process.

Dataset S4. The interaction items evaluation between RIG-I and TRIM25.

Dataset S5. STRING interactions matrix of RIG-I related gene cluster.

References

1. Szklarczyk D, *et al.* (2019) STRING v11: protein-protein association networks with increased coverage, supporting functional discovery in genome-wide experimental datasets. *Nucleic acids research* 47(D1):D607-d613.
2. Wang P, *et al.* (2014) The STAT3-binding long noncoding RNA lnc-DC controls human dendritic cell differentiation. *Science* 344(6181):310-313.
3. Yisraeli JK & Melton DA (1989) Synthesis of long, capped transcripts in vitro by SP6 and T7 RNA polymerases. *Methods in enzymology* 180:42-50.
4. Mukherjee K, Korithoski B, & Kolaczkowski B (2014) Ancient origins of vertebrate-specific innate antiviral immunity. *Molecular biology and evolution* 31(1):140-153.
5. Sun HM, *et al.* (2017) PALLD Regulates Phagocytosis by Enabling Timely Actin Polymerization and Depolymerization. *Journal of immunology* 199(5):1817-1826.
6. Jiang LJ, *et al.* (2011) RA-inducible gene-I induction augments STAT1 activation to inhibit leukemia cell proliferation. *Proceedings of the National Academy of Sciences of the United States of America* 108(5):1897-1902.